

# NLRP3 Inflammasome Deficiency Alleviates Inflammation and Oxidative Stress by Promoting PINK1/Parkin-Mediated Mitophagy in Allergic Rhinitis Mice and Nasal Epithelial Cells

Hong Ding<sup>1</sup>, Xiaofan Lu<sup>2</sup>, Huimin Wang<sup>3</sup>, Wenming Chen<sup>3</sup>, Bing Niu<sup>4</sup>

<sup>1</sup>Otolaryngology Department, The Second Clinical Medical College, Henan University of Chinese Medicine, Zhengzhou, Henan Province, People's Republic of China; <sup>2</sup>Respiratory Department, The Second Clinical Medical College, Henan University of Chinese Medicine, Zhengzhou, Henan Province, People's Republic of China; <sup>3</sup>Otolaryngology Department, Henan Provincial Hospital of Traditional Chinese Medicine, Zhengzhou, Henan Province, People's Republic of China; <sup>4</sup>Stomatology Department, Henan Provincial Hospital of Traditional Chinese Medicine, Zhengzhou, Henan Province, People's Republic of China

Correspondence: Hong Ding; Bing Niu, Henan University of Chinese Medicine, The Second Clinical Medical College, 6 Dongfeng Road, Jinshui District, Zhengzhou City, Henan Province, 450002, People's Republic of China, Email superding@hactcm.edu.cn; 13838061768@163.com

**Purpose:** Accumulating evidence indicates that oxidative stress and inflammation are the pathological basis of allergic diseases. Inhibition of NOD-like receptor family pyrin domain-containing 3 (NLRP3) inflammasome could ameliorate allergic rhinitis (AR). Here, we explored the effects and mechanisms that underlie NLRP3 inhibition on oxidative stress and inflammation in AR.

**Methods:** Ovalbumin (OVA)-induced AR murine model was established using wild-type (WT) and NLRP3-deficient mice. HNEpCs were stimulated with interleukin (IL)-13 with MCC950 pretreatment or PTEN-induced putative kinase 1 (PINK1) siRNA. The indicators of oxidative stress, inflammation, apoptosis, and mitophagy were determined both in vivo and in vitro.

**Results:** NLRP3 knockout (KO) reduced the frequency of nasal rubbing and sneezing, the infiltration of eosinophils, the number of mast cells, and the accumulation of goblet cells in AR mice after OVA stimulation. The NLRP3 KO AR mice exhibited the increased concentrations of OVA-specific immunoglobulin E (OVA-sIgE), IL-1 $\beta$ , IL-4, IL-13, IL-6, TNF- $\alpha$ , and the upregulated level of IFN- $\gamma$ . NLRP3 KO significantly inhibited oxidative stress, and also markedly decreased apoptosis in the nasal mucosa of AR mice. Moreover, evaluated protein expressions of PINK1, enzyme 3 (E3) ubiquitin ligase PRKN (Parkin), and LC3 II, decreased expression of TOM20, as well as the increased colocalization of LC3 with mitochondria were observed in NLRP3 KO AR mice. In vitro, IL-13 exposure increased the levels of NLRP3 and IL-1 $\beta$ . Inhibition of NLRP3 using MCC950 enhanced PINK1/Parkin-mediated mitophagy but attenuated inflammation, oxidative stress, and apoptosis. However, PINK1 knockdown abrogated mitophagy and also reversed the protective effects of MCC950 on inflammation, oxidative stress, and apoptosis in HNEpCs stimulated with IL-13.

**Conclusion:** Inhibition of NLRP3 inflammasome exerts the protective effects on AR by facilitating mitophagy regulated by PINK1/Parkin signaling pathway.

**Keywords:** NLRP3, mitophagy, inflammation, oxidative stress, PINK1/Parkin

## Introduction

As an allergic inflammatory disease of the nasal mucosa, allergic rhinitis (AR) is driven by immunoglobulin E (IgE)-mediated reactions when exposure to allergens. The typical symptoms of AR included sneezing, itchy nose, runny nose, and nasal congestion. Moreover, some patients even have clinical manifestations such as skin itching, cough, and eye itching.<sup>1</sup> AR is a disease characterized by a high incidence in both adults and children. It confers a huge health burden and influences the quality of people's life severely. Due to its prevalence, AR has a great impact on our economic through acting on productivity, the use of healthcare resources, and education.<sup>2,3</sup> However, the pathogenesis of AR has not yet

been fully elucidated. Therefore, elucidating the molecular mechanisms of AR may open a window on new management strategies.

NOD-like receptor family pyrin domain-containing 3 (NLRP3) inflammasome is an important component of the innate immunity system. In recent years, the abnormal activation of NLRP3 inflammasome has been reported to be closely correlate with AR.<sup>4</sup> The activation of NLRP3 inflammasome in AR can facilitate the production and the release of interleukin-1 $\beta$  (IL-1 $\beta$ ) and IL-18, thus initiating a cascade of inflammation, ultimately promoting the development of AR.<sup>5,6</sup> The NLRP3 inflammasome can be activated by multiple cellular and molecular events, as well as diverse stimuli. Among them, reactive oxygen species (ROS) is regarded as the common signal for the activation of NLRP3 inflammasome.<sup>7</sup>

Mitochondria act as the vital organelle with a variety of functions and are also the major source of ROS via their respiratory functions.<sup>8</sup> The increased generation of mitochondrial ROS (mtROS) from the damaged mitochondria participates in the NLRP3 inflammasome activation.<sup>9,10</sup> Mitochondria-selective autophagy (mitophagy) plays a central role in maintaining mitochondrial homeostasis by eliminating the damaged mitochondria.<sup>11</sup> To initiate mitophagy, PTEN-induced putative kinase1 (PINK1) stabilizes the outer mitochondrial membrane to recruit the enzyme 3 (E3) ubiquitin ligase PRKN (Parkin) from cytosol to the damaged mitochondria, ultimately removing unhealthy mitochondria through the autophagy machinery.<sup>12</sup> Previously, Liu et al demonstrated that PINK1/Parkin-mediated mitophagy can inhibit apoptosis and NLRP3 inflammation activation in AR.<sup>13</sup> Notably, emerging evidence suggested that mitophagy can be controlled by NLRP3 inflammasome.<sup>14</sup> However, the role of NLRP3 inflammasome activation on mitophagy in AR is still unclear. Hence, the aim of this study was to explore the effect of NLRP3 inflammasome in mediating mitophagy using the AR mouse model and IL-13 treated HNEpCs.

## Material and Methods

### Animal and AR Mice Model

NLRP3 knockout (KO, NLRP3<sup>-/-</sup>) and wild type (WT) female C57BL/6 mice were obtained from Jackson Laboratory (Sacramento, CA, USA). Mice were housed under the pathogen-free conditions and received free access to standard rodent chow and water. All mice were acclimated for 7 days before the experiment. The experimental procedures were carried out in accordance with the National Institutes of Health (NIH) Guide for the Care and Use of Experimental Animals, and all protocols for animal studies were approved by the Ethics Committee of Henan University of Chinese Medicine (PZ-HNSZY-2021-041).

A total of 36 mice were randomly divided into 3 groups: control (WT mice), AR (WT mice), AR+NLRP3<sup>-/-</sup>. Mice in AR and AR+NLRP3<sup>-/-</sup> groups were intraperitoneally injection of 300  $\mu$ L phosphate buffer saline (PBS) containing 100  $\mu$ g ovalbumin (OVA, Sigma-Aldrich, St. Louis, MO, USA) and 1 mg aluminum hydroxide (Sigma-Aldrich) on days 0, 7, and 14. On days 21–27, mice were challenged with 20  $\mu$ L PBS containing 200  $\mu$ g OVA by means of intranasal instillation (10  $\mu$ L per nostril). Mice in the control group were injected and challenged with PBS at the same dose.

### Evaluation of Nasal Symptoms

The frequencies of nasal rubbing and sneezing were counted to evaluate the allergic symptoms. The data were recorded by three blinded observers within 15 min after the last OVA stimulation.

### Enzyme Linked Immunosorbent Assay (ELISA)

Mice were anesthetized with sodium pentobarbital (intraperitoneal injection, 50 mg/kg). The collected blood was left under room temperature for 60 min. After centrifugation (4°C, 3000 rpm), the supernatant was harvested. The levels of OVA-specific immunoglobulin E (OVA-sIgE), interleukin (IL)-1 $\beta$  (IL-1 $\beta$ ), IL-4, IL-6, IL-13, tumor necrosis factor  $\alpha$  (TNF- $\alpha$ ), and Interferon  $\gamma$  (IFN- $\gamma$ ) were determined by ELISA kits (Bioswamp, Wuhan, China) using a microplate reader (PerkinElmer, Waltham, MS, USA).

## Histopathological Analysis

Nasal mucosal tissues were fixed in paraformaldehyde (4%) for 24 h and then decalcified with EDTA solution (Solarbio, Beijing, China) for 10–12 days. Next, the nasal tissues were embedded in paraffin and cut into sections (5  $\mu\text{m}$  thickness). The sections were stained with hematoxylin-eosin (HE, for eosinophils and the morphology of nasal tissues), toluidine blue (TB, for mast cells), and periodic acid-Schiff (PAS, for goblet cells) reagents (All from Solarbio, Beijing, China) according to the manufacturer's instructions. Images were captured using a Panoramic MIDI Digital pathology scanning system (3D HISTECH; Budapest, Hungary). The numbers of eosinophils, mast cells, and goblet cells were counted as number/ $\text{mm}^2$  (per section).

## Cell Culture, Treatment, and siRNA Transfection

Human nasal epithelial cell line (HNEpCs, BeNa Culture Collection, Beijing, China) was cultured in EMEM complete medium (BeNa Culture Collection) at 37°C in a humidified atmosphere with 5%  $\text{CO}_2$ .

HNEpCs were stimulated with recombinant IL-13 (10 ng/mL, STEMCELL, Vancouver, Canada) for 24 h as described previously.<sup>13</sup> To inhibit the activation of NLRP3 inflammasome, HNEpCs cells were pre-treated with 10  $\mu\text{M}$  MCC950 (Sigma-Aldrich) for 1 h before IL-13 exposure.

HNEpCs were transfected with negative control (NC) siRNA or PINK1 siRNA (Thermo Fisher) duplexes using Lipofectamine RNAiMAX Reagent (Invitrogen, Carlsbad, CA, USA) according to use instruction strictly. To generate the siRNA-lipid complexes, the transfection medium (200  $\mu\text{L}$ ) containing transfection reagent (10  $\mu\text{L}$ ) was gently mixed with 200  $\mu\text{L}$  transfection medium containing NC siRNA or PINK1 siRNA, and then kept at room temperature for 15 min. When the cell confluence reached at 40–60%, cells were transfected with siRNA-lipid complexes for 24 h and then stimulated with MCC950 or IL-13 as described above. The working concentration of PINK1 siRNA is 100 pmol.

## Detection of Oxidative Stress

Tissue and cell samples were collected and centrifuged at 4000 rpm at 4°C for 15 min. The protein concentration was quantified using the BCA protein assay kit (Biorab, Beijing, China). The level of glutathione (GSH), the content of malondialdehyde (MDA), and the activity of superoxide dismutase (SOD) were determined using the commercial kits (Biorab).

## Measurement of Mitochondrial Reactive Oxygen Species (mtROS)

After treatment, the mtROS level in HNEpCs was assessed using MitoSOX (Thermo Fisher Scientific). HNEpCs were incubated with 5  $\mu\text{M}$  MitoSOX dye for 20 min at 37°C in the dark. The images were captured using the Cytation 5 imaging system (BioTek, Winooski, VT, USA). Evaluation of nasal symptoms.

## Western Blot

The nasal tissues and cells were lysed in RIPA Lysis Buffer (Beyotime, Shanghai, China) containing the protease inhibitor cocktail (Servicebio). The total protein concentration was determined with BCA kit (Biorab). Proteins (25  $\mu\text{g}$ ) were separated using SDS-PAGE (10–15% gels), and then transferred onto a PVDF membrane (Millipore, Billerica, MA, USA). The membranes were blocked in 5% skim milk at room temperature for 1 h, and incubated at 4°C overnight, with the following primary antibodies: NLRP3 (68102-1-Ig, PROTEINTECH, Wuhan, China), BCL2 associated X protein (Bax, AF0120, AFFINITY, Jiangsu, China), B-cell CLL/lymphoma 2 (Bcl-2, AF6139, AFFINITY), PINK1 (DF7742, AFFINITY), Parkin (66674-1-Ig, PROTEINTECH), LC3 (SAB1305552, Sigma-Aldrich), outer mitochondrial membrane receptor Tom20 (TOM20, 11802-1-AP, PROTEINTECH), and GAPDH (10494-1-AP, PROTEINTECH). Subsequently, the membranes were incubated with secondary horseradish peroxidase-conjugated goat anti-mouse antibody (5257, Cell Signaling Technology, Danvers, MA, USA) or HRP-goat anti-rabbit antibody (5151, Cell Signaling Technology) for 1 h at room temperature. Finally, the bands were visualized using an enhanced chemiluminescent reagent (WBKLS0500, Millipore) and quantified using the ImageJ software (version 1.44, National Institutes of Health, Bethesda, MD, USA).

## Terminal Deoxynucleotidyl Transferase dUTP Nick End Labeling (TUNEL) Assay

The apoptotic cells death in nasal mucosa tissues and HNEpCs were determined using the One Step TUNEL detection kit (Beyotime) according to the manufacturer's protocol. The numbers of TUNEL-positive cells and nuclei (DAPI, blue) were counted, respectively. The percentage of TUNEL-positive cells were obtained by dividing the number of TUNEL-positive nuclei by the number of nuclei times 100.

## Immunofluorescence (IF)

For antigen repair, the slices were retrieved by citric acid buffer (0.01 M, pH6.0) and heated in a microwave oven. The slices were cooled to room temperature and rinsed 3 times with PBS. The samples were incubated with primary antibodies against LC3 (SAB1305552, Sigma-Aldrich) and COX IV (11242-1-AP, PROTEINTECH) overnight at 4°C. Subsequently, the slices were probed with with the corresponding secondary antibodies [Cy3-conjugated Goat Anti-Mouse IgG(H+L) (SA00009-1) or CoraLite488-conjugated Goat Anti-Rabbit IgG(H+L) (SA00013-2)] for 1 h at room temperature in the dark. Finally, the nuclei were stained with DAPI. The fixed HNEpCs were immunostained with the corresponding primary antibodies against NLRP3 (68102-1-Ig, PROTEINTECH), IL-1 $\beta$  (16806-1-AP, PROTEINTECH), LC3 (SAB1305552, Sigma-Aldrich), Parkin (66674-1-Ig, PROTEINTECH), and COX IV (11242-1-AP, 1:100, PROTEINTECH). The cells were washed 3 times with PBS, and then incubated with the appropriate amount of secondary antibodies. The images were captured using a fluorescence microscope (Nikon Corporation).

## Immunohistochemistry (IHC)

The IHC assay was performed as previously described with a minor modification.<sup>15</sup> The samples were incubated with a primary antibody against c-Caspase-3 (AF7022, 1:100, AFFINITY) overnight at 4 °C, and then with the biotinylated goat anti-rabbit antibody (BA1003, 1:100, Boster, Wuhan, China) at room temperature for 60 min. The activity of peroxidase was visualized by 3, 3'-diamino-benzidine tetrahydrochloride (DA1010, Solarbio) for 5 min. The images were captured with Panoramic MIDI Digital pathology scanning system and evaluated using Image J software.

## Statistical Analysis

All the data were performed using SPSS software (version 22.0; IBM Co., Armonk, NY, USA). All values are presented as the mean  $\pm$  standard error of the mean (SEM). The Student's *t*-test was used to determine the differences between the two groups. One-way Analysis of variance (ANOVA) and Tukey's post-hoc test were used to determine the differences among groups. *P* value less than 0.05 was considered statistically significant.

## Results

### NLRP3 Deficiency Alleviates OVA-Induced AR in Mice

AR mice model was established as illustrated in Figure 1A. As presented in Figure 1B and C, the protein level of NLRP3 in AR group was notably upregulated, compared with those in control group. NLRP3 knockout blocked the upregulation of NLRP3 induced by OVA. Compared with control group, the frequencies of nasal rubbing and sneezing were higher in the AR group. However, the frequencies of nasal rubbing and sneezing in NLRP3<sup>-/-</sup> AR mice were lower than those in wild-type (WT) AR mice (Figure 1D and E). In addition, the levels of serum OVA-sIgE in AR+ NLRP3<sup>-/-</sup> group was lower compared with that in control group (Figure 1F). As illustrated in Figure 1G–K, the nasal mucosa of AR mice exhibited the numerous eosinophils, cilia shedding, goblet cell hyperplasia. Furthermore, the number of mast cells were significantly higher in WT AR mice compared with that in control group. By contrast, NLRP3 KO alleviated these histopathological changes. These findings indicated that NLRP3 KO relieved the nasal symptoms and restored the histopathological changes in OVA-induced AR mice.

### NLRP3 KO Attenuates Oxidative Stress, Inflammatory Response and Apoptosis in AR Mice

Next, oxidative stress and inflammation in control, AR, and AR-NLRP3<sup>-/-</sup> mice were examined. As shown in Figure 2A–C, OVA decreased the activity of SOD and the level of GSH, but increased the level of MDA in nasal

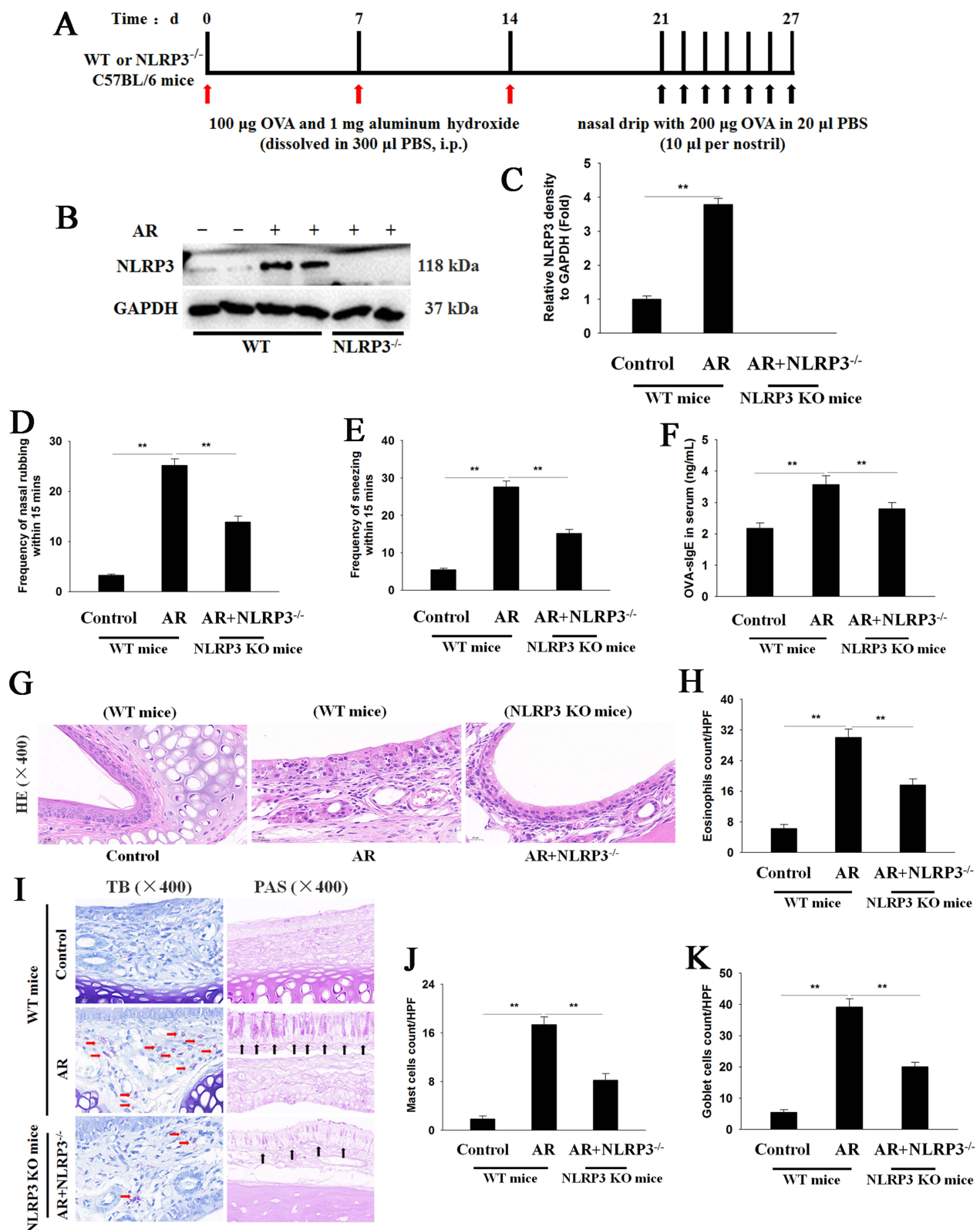


**Figure 1** NLRP3 KO attenuated the allergy-like nasal symptoms and histopathological changes in OVA-induced AR mice. **(A)** Schematic diagram of AR. **(B and C)** Western blot analysis and quantification of NLRP3. **(D and E)** Comparison of the frequencies of nasal rubbing and sneezing in each group within 15 min. **(F)** The concentration of OVA-sIgE in serum was detected by ELISA. **(G–K)** Representative images and the quantification of eosinophils (determined by HE staining), mast cells (red arrow, determined by TB staining), and goblet cells (black arrow, determined by PAS staining). Magnification: 400×. Data are presented as mean ± SEM (n=6 mice per group). \*\*P<0.01.

**Abbreviations:** WT, wild type; KO, knockout; AR, allergic rhinitis; NLRP3, NOD-like receptor family pyrin domain-containing 3; ELISA, enzyme linked immunosorbent assay; OVA-sIgE, OVA-specific immunoglobulin E; HE, hematoxylin-eosin; TB, toluidine blue; PAS, periodic acid-Schiff.

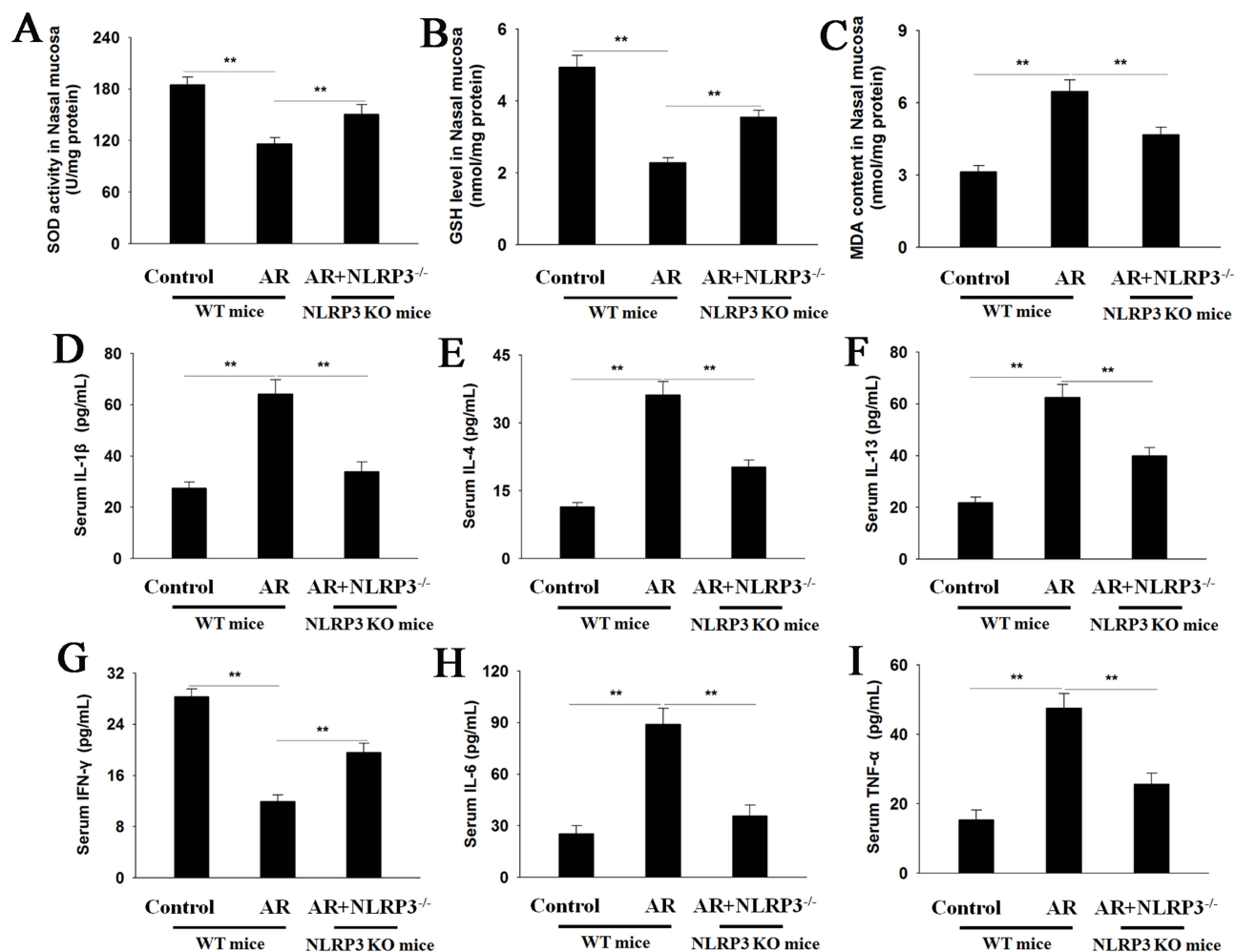


**Figure 2** NLR3 KO inhibits oxidative stress and inflammation in OVA-induced AR mice. The changes of SOD activity (A), GSH level (B), and MDA content (C) were determined in nasal mucosa. (D–I) ELISA assays for serum IL-1 $\beta$ , IL-4, IL-13, IFN- $\gamma$ , IL-6, and TNF- $\alpha$ . Data are presented as mean  $\pm$  SEM (n=8 per group). \*\*P<0.01. **Abbreviations:** WT, wild type; KO, knockout; AR, allergic rhinitis; ELISA, enzyme linked immunosorbent assay.

mucosa in comparison to those in control. AR mice exhibited higher levels of IL-1 $\beta$ , IL-4, IL-13, IL-6, and TNF- $\alpha$  and a lower level of IFN- $\gamma$  (Figure 2D–I). However, NLR3 KO markedly attenuated oxidative stress and inflammation in AR mice.

As shown in Figure 3A and B, NLR3 KO restored Bcl-2 expression that was suppressed by OVA whilst reversing OVA-induced upregulation of Bax expression. The TUNEL assay revealed that the TUNEL-positive cells in AR +NLR3<sup>-/-</sup> group was lower than that in WT AR mice (Figure 3D and E). Consistent with the result of TUNEL assay, IHC staining revealed that NLR3 KO inhibited the expression of c-Caspase-3 (a pro-apoptotic protein) in nasal mucosa of AR mice (Figure 3E and F). These results indicated that NLR3 deficiency inhibits oxidative stress, inflammatory reaction, and apoptosis in AR mice.

## NLR3 KO Promotes PINK1/Parkin-Mediated Mitophagy in AR Mice

Next, the effect of NLR3 KO on PINK1/Parkin-mediated mitophagy in AR mice was investigated. The protein levels of PINK1, Parkin, and LC3 II in nasal mucosa of NLR3<sup>-/-</sup> AR mice were higher than those in the WT AR mice (Figure 4A–E). While the protein level of TOM20 in nasal mucosa of NLR3<sup>-/-</sup> AR mice was lower than that in the WT AR mice (Figure 4A and D). The result of IF analysis indicated that the NLR3<sup>-/-</sup> AR mice exhibited the upregulated co-localization of LC3 with COX IV (Figure 4F). This data showed that NLR3 deficiency promoted the formation of mitophagosomes in nasal mucosa of AR mice.

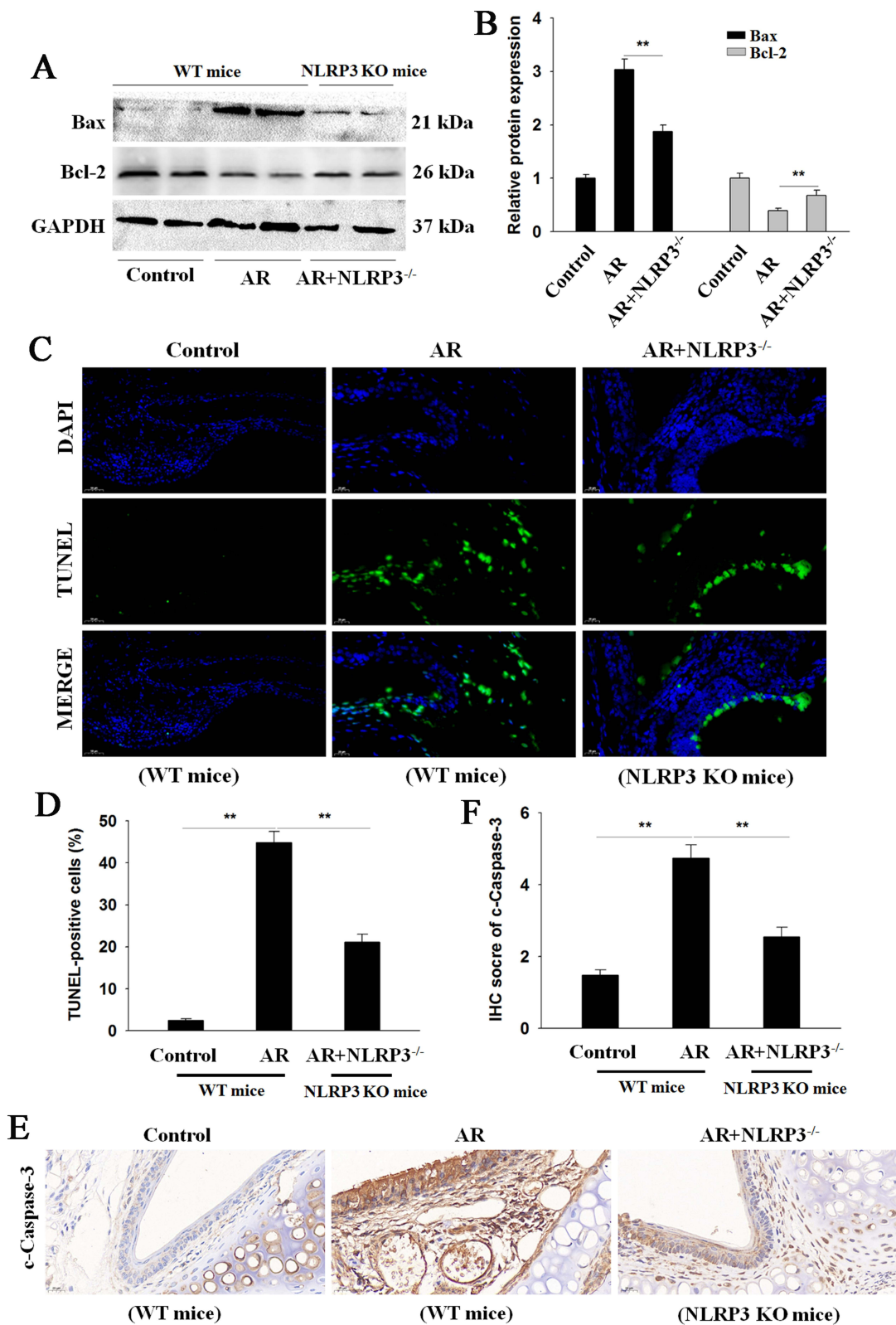


**Figure 3** NLRP3 KO alleviates apoptosis in OVA-induced AR mice. **(A and B)** Western blot analysis and quantification of Bax and Bcl-2 in nasal mucosa tissue extracts. **(C and D)** Apoptosis was evaluated by TUNEL assay. Magnification: 400 $\times$ . **(E and F)** Representative IHC images and quantification of c-Caspase-3 in nasal mucosa tissues. Magnification: 400 $\times$ . Data are presented as mean  $\pm$  SEM (n=5 per group). \*\*P<0.01.

**Abbreviations:** WT, wild type; KO, knockout; AR, allergic rhinitis; NLRP3, NOD-like receptor family pyrin domain-containing 3; TUNEL, terminal deoxynucleotidyl transferase dUTP nick end labeling.

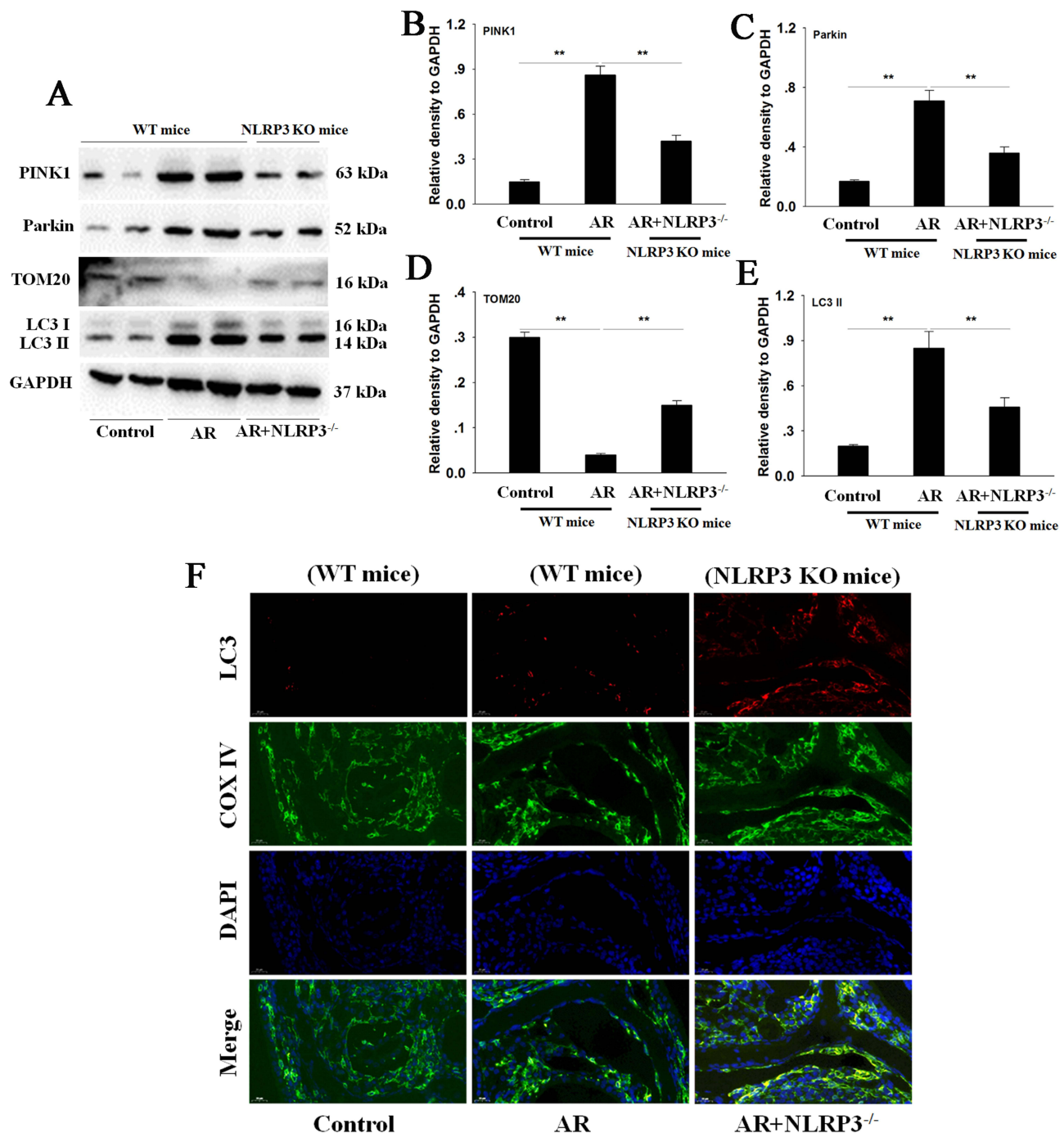


**Figure 4** NLRP3 KO promotes PINK1/Parkin-mediated mitophagy in OVA-induced AR mice. (A–E) Western blot analysis and quantification of PINK1, Parkin, TOM20, and LC3 II levels in nasal mucosa tissue extracts. (F) Mitophagosomes were evaluated by COX IV (mitochondria) and LC3. Magnification: 400 $\times$ . Data are presented as mean  $\pm$  SEM (n=5 per group). \*\*P<0.01.

**Abbreviations:** WT, wild type; KO, knockout; AR, allergic rhinitis; NLRP3, NOD-like receptor family pyrin domain-containing 3.

## Effects of MCC950 on the Levels of NLRP3, IL-1 $\beta$ , and Mitophagy in IL-13-Exposed HNEpCs

The results of IF analysis indicated that the levels of NLRP3 and IL-1 $\beta$  were significantly increased in HNEpCs stimulated with IL-13. MCC950 pretreatment inhibited the upregulation of NLRP3 and IL-1 $\beta$  induced by IL-13 in HNEpCs (Figure 5A–C). As shown in Figure 5D–H, the IL-13-treated HNEpCs pretreated with the MCC950 (a NLRP3 inhibitor) showed the enhanced levels of PINK1, Parkin, and LC3 II, and decreased level of TOM20.

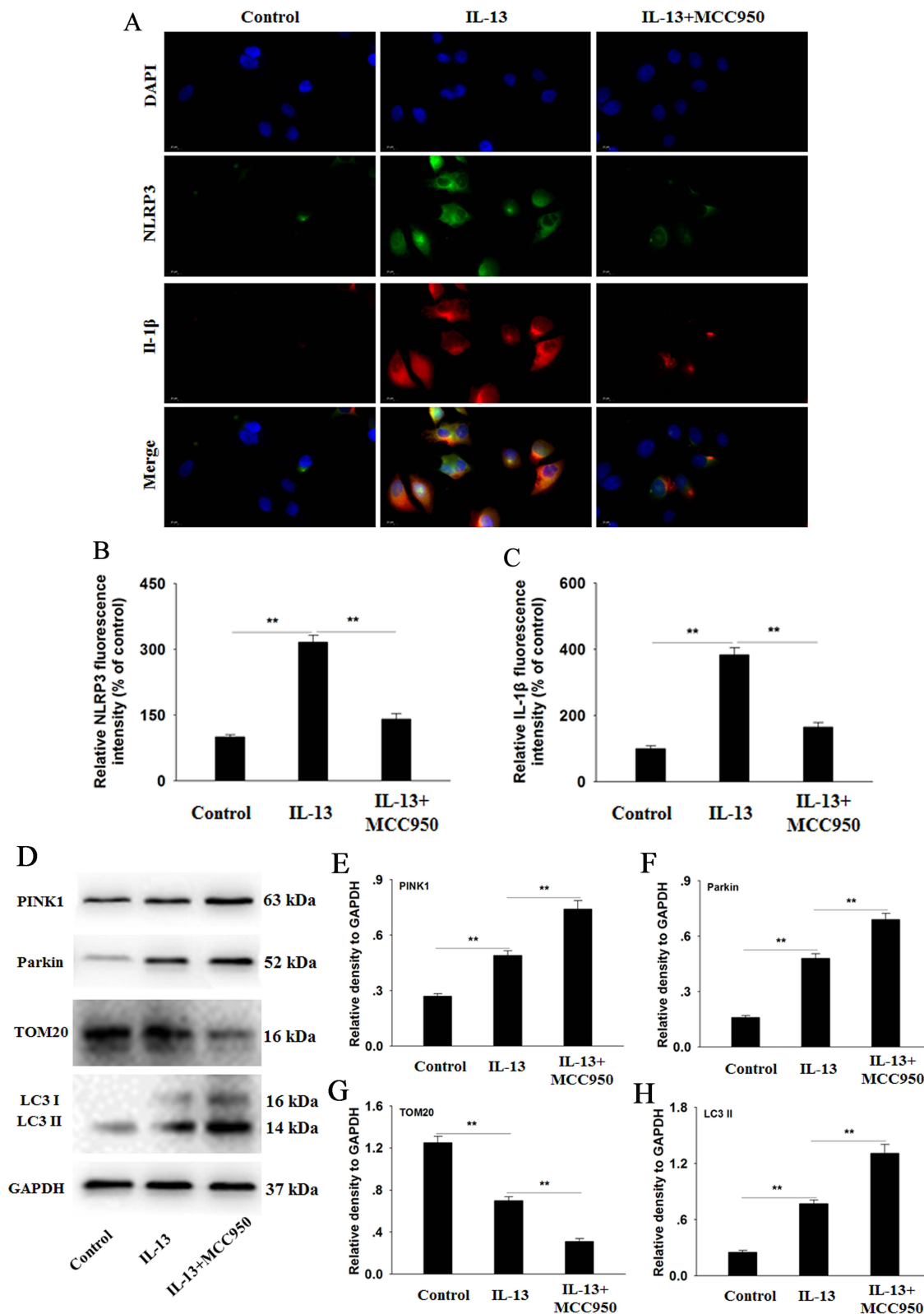


**Figure 5** Effects of MCC950 on NLRP3 inflammasome and mitophagy in IL-13-stimulated HNEpCs. HNEpCs were pretreated with 10  $\mu$ M MCC950 for 1 h and then incubated with IL-13 (10 ng/mL) for 24 h. **(A)** Representative images of NLRP3 and IL-1 $\beta$  in each group (Magnification: 400 $\times$ ). **(B and C)** The quantification of NLRP3 and IL-1 $\beta$  immunofluorescent staining in HNEpCs. **(D–H)** Western blot analysis and quantification of PINK1, Parkin, LC3, and TOM20 in HNEpCs. Data are presented as mean  $\pm$  SEM (n=3). \*\*P<0.01.

## MCC950 Inhibits Oxidative Stress, Inflammation, and Apoptosis via Upregulating PINK1-Dependent Mitophagy in IL-13-Stimulated HNEpCs

As presented in Figure 6A–E, the results of Western blot analysis indicated that PINK1 siRNA decreased the protein levels of PINK1, Parkin, and LC3 II in IL-13-stimulated HNEpCs pretreated with MCC950. Furthermore, PINK1 siRNA mitigated the reduced level of TOM20 in HNEpCs in response to IL-13 and MCC950. IF analysis also confirmed that PINK1 siRNA inhibited the co-localization of Parkin with COX IV in HNEpCs treated with IL-13 and MCC950 (Figure 6F).

Pretreatment with MCC950 inhibited the IL-13-induced enhanced levels of IL-6 and TNF- $\alpha$  (Figure 7A and B). As shown in Figures 7C–E, MCC950 reversed the IL-13-induced increase in mtROS and MDA levels in HNEpCs. Additionally, MCC950 was demonstrated to restore SOD activity and GSH level that were previously inhibited by IL-13 in HNEpCs (Figure 7F and G). The proportion of TUNEL-positive HNEpCs markedly reduced in IL-13-treated HNEpCs with MCC950 pretreatment (Figure 7H and I). However, PINK1 siRNA attenuated the protective effects of MCC950 on inflammation, oxidative damage, and apoptosis in IL-13-treated HNEpCs. Overall, these results suggested that inhibition of NLRP3 inflammasome can inhibit IL-13-induced inflammation, oxidative damage, and apoptosis through PINK1/Parkin-mediated mitophagy in HNEpCs.

## Discussion

OVA-induced AR mice model can exactly mimic the characteristic symptoms of AR (sneezing and scratching). Furthermore, OVA-induced AR mice model is suitable for exploring the effect of NLRP3 inflammasome on the pathogenesis of AR.<sup>16</sup> Inhibiting the activation of NLRP3 inflammasome can effectively release AR symptoms.<sup>17,18</sup> In this study, we found that the levels of NLRP3 was upregulated in nasal mucosa of OVA-induced AR mice. NLRP3 KO alleviated nasal symptoms and relieved histopathological changes in OVA-induced AR mice. Increasing evidence suggested that the imbalance of Th1/Th2 ratio plays an essential role in AR development.<sup>19,20</sup> AR is generally considered as a Th2 cells-driven disease, the decreased level of Th1 cytokine (eg, IFN- $\gamma$ ) and the increased levels of Th2 cytokines (eg, IL-4 and IL-13) are critical for hypersensitivity of nasal mucosa.<sup>21,22</sup> IgE-specific antibodies (sIgE) are anchored on the surface of mast cells or exist in the blood in free form. The allergens are recognized by sIgE antibodies and then trigger the nasal mucosal inflammatory reactions.<sup>23,24</sup> In this study, we found that NLRP3 KO increased the level of IFN- $\gamma$  and decreased the levels of IL-4 and IL-13 in AR mice. Moreover, the nasal symptoms were alleviated and the level of OVA-sIgE was decreased in NLRP3<sup>-/-</sup> AR mice. These data indicated that inhibiting the activation of NLRP3 inflammasome reversed the imbalance between the ratio of Th1 and Th2 in AR mice.

Inflammation cells are involved in AR development.<sup>25</sup> The accumulation of IL-13 and IL-4 promotes the production of sIgE antibodies that interact with the receptors on the surface of mast cells to release the allergenic mediators, ultimately inducing the release of chemokines and pro-inflammatory cytokines (IL-6, IL-1 $\beta$ , and TNF- $\alpha$ ).<sup>26</sup> IL-1 $\beta$ , IL-6, and TNF- $\alpha$  are the important pro-inflammatory factors associated with AR.<sup>27</sup> As AR progresses, the infiltration of eosinophils and the hyperplasia of goblet cells can further promote AR development.<sup>28</sup> In the current study, we found that NLRP3 KO decreased the numbers of mast cells, eosinophils, and goblet cells as well as IL-1 $\beta$ , IL-6, and TNF- $\alpha$  levels in OVA-induced AR mice.

Oxidative stress is closely related to various pathological and physiological processes. Excessive consumption of antioxidant system cannot effectively scavenge free radicals, thus resulting in the disruption of molecular signaling pathways and tissue injury.<sup>29</sup> Oxidative stress in AR has attracted extensive attention, and antioxidant therapy has been used to improve the symptoms and signs in AR patients.<sup>30,31</sup> A recent study suggested the crucial role of oxidative stress in NLRP3 inflammasome activation. Increased ROS level results in the activation of NLRP3/IL-1 $\beta$  signaling pathway, and pretreatment with Mito-TEMPO or N-acetyl-L-cysteine blocked the upregulated levels of NLRP3 and IL-1 $\beta$ .<sup>32,33</sup> The current study found that NLRP3 KO attenuated OVA-induced increase in MDA content and reversed the inhibitory effects of OVA on SOD activity and GSH level. The apoptosis caused by exorbitant oxidative stress triggers plays an important role in the progression of AR.<sup>34</sup> Our results showed that NLRP3 KO effectively prevented the apoptosis in nasal mucosa tissue and in OVA-induced AR mice.

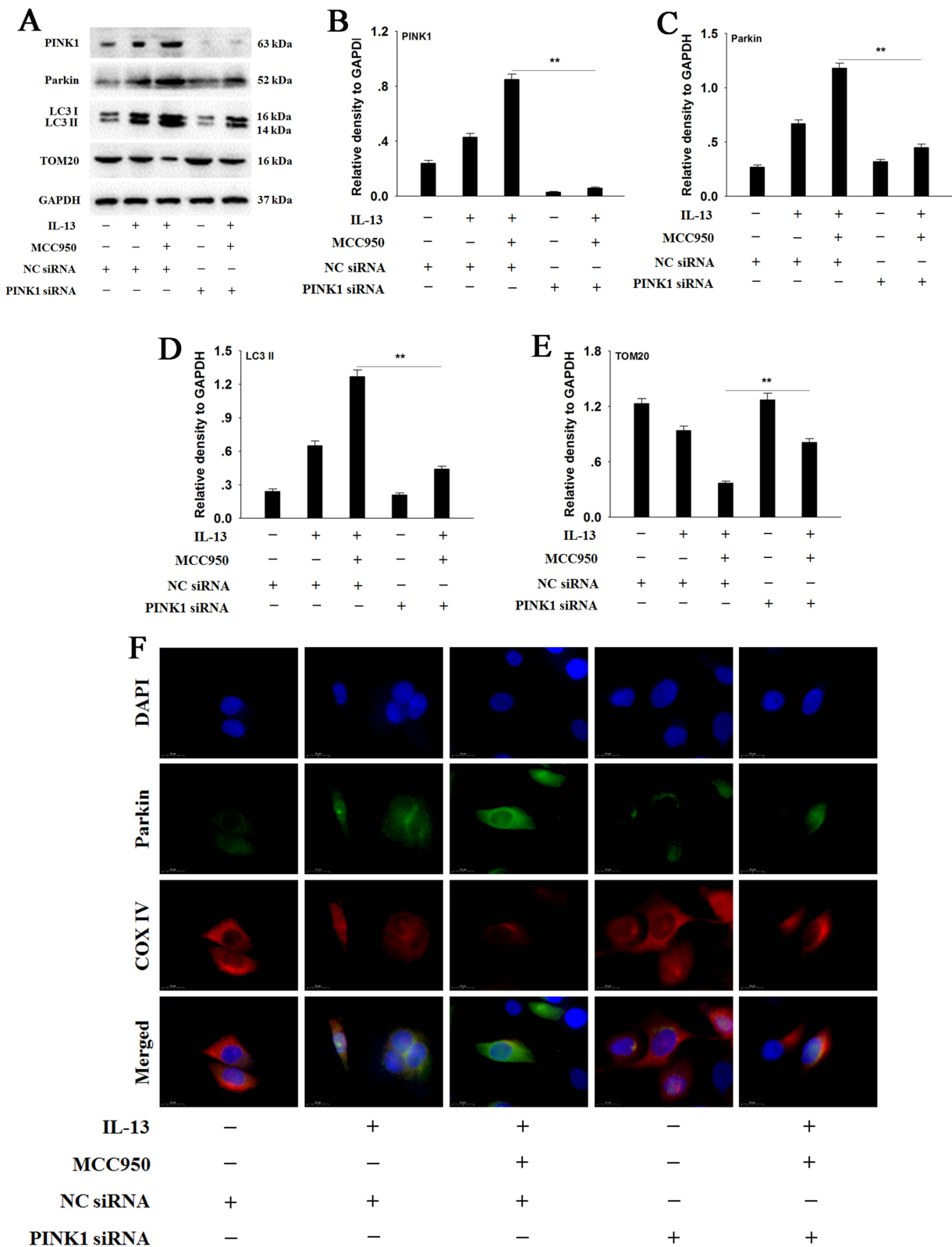


**Figure 6** NLRP3 inhibition enhances PINK1/Parkin-mediated mitophagy in IL-13 treated HNEpCs. HNEpCs were transfected with NC siRNA or PINK1 siRNA, and then added the remaining reagents in order. **(A–E)** Western blot analysis and quantification of PINK1, Parkin, LC3, and TOM20 in HNEpCs. **(F)** The co-localization of Parkin (green) with COX IV (red) were determined by IF analysis. Magnification: 400×. Data are presented as mean ± SEM (n=3). \*\*P<0.01. **Abbreviations:** NC, negative control; IF, immunofluorescence.

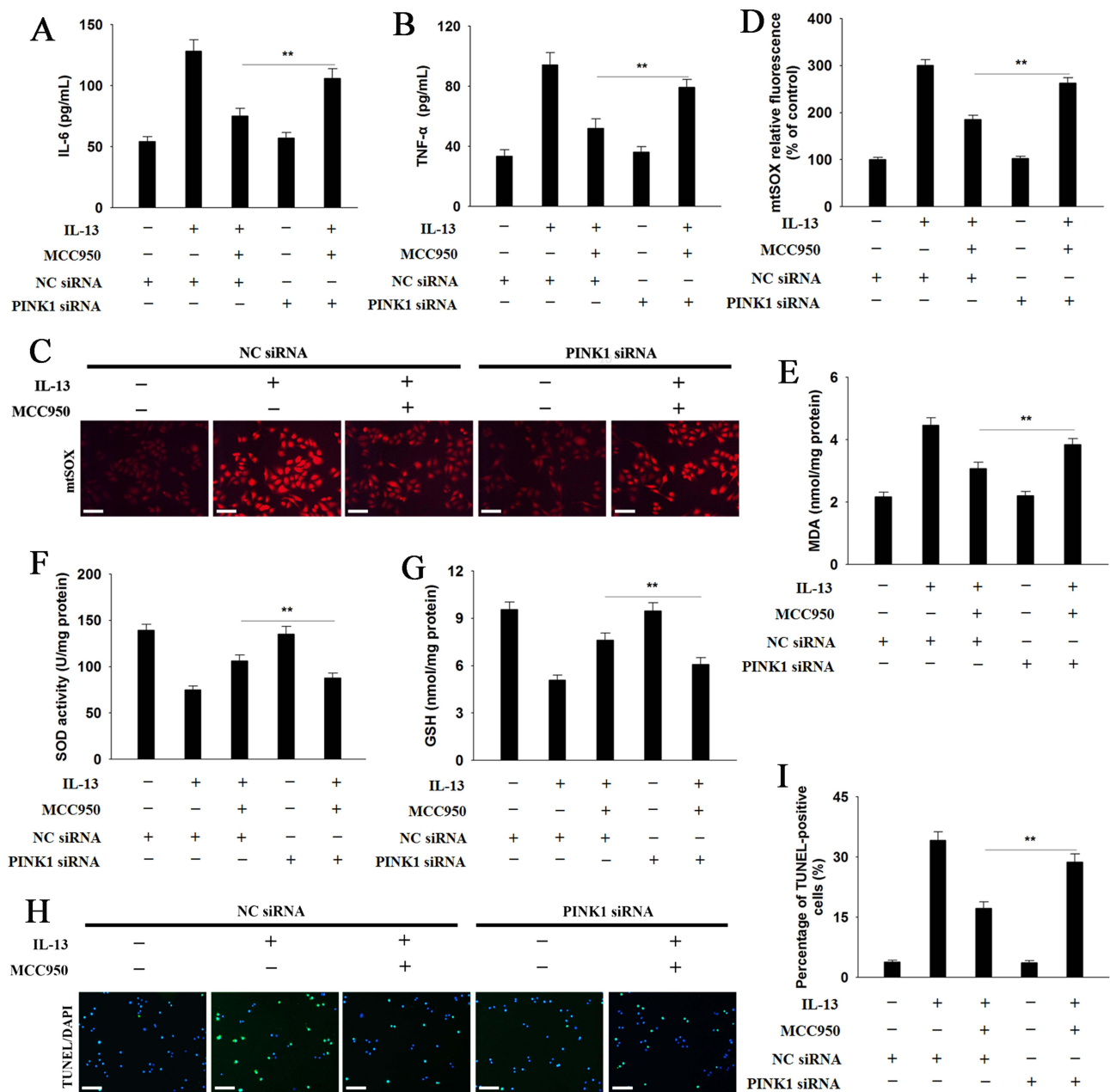


**Figure 7** PINK1 siRNA attenuates the protective effects of MCC950 on IL-13 treated HNEpCs. **(A and B)** The levels of IL-6 and TNF- $\alpha$  were determined by the ELISA kits. **(C and D)** Representative micrographs of mtROS were indicated by MitoSOX staining and the integrated fluorescence intensity was quantified (Magnification: 200 $\times$ ). **(E–G)** MDA content, SOD activity, GSH level were determined. **(H and I)** Representative immunofluorescence images and quantification of TUNEL-positive cells in HNEpCs (Magnification: 100 $\times$ ). Data are presented as mean  $\pm$  SEM (n=3). \*\* $P$ <0.01.

Mitochondria have multiple functions such as cell survival/death signaling, ROS signaling, calcium buffering, and steroid hormone biosynthesis. Cells have a series of processes related to mitochondrial quality control to maintain mitochondrial functionality and integrity.<sup>35</sup> Mitochondria can initiate mitophagy to clear the damaged mitochondria via autophagosome-lysosome pathway. The induction of mitophagy limits the overproduction of ROS and maintains the mitochondrial homeostasis.<sup>36</sup> An accumulating body of research indicates there is a relationship between mitophagy and NLRP3 inflammasome.<sup>37</sup> Polydatin exerts the protective effect on AR via activating PINK1/Parkin-mediated mitophagy.<sup>13</sup> PINK1/Parkin-mediated prevented tissue injury and apoptosis in contrast-induced acute kidney injury via inhibiting NLRP3 inflammasome activation.<sup>38</sup> Notably, mitophagy were negatively correlated with the NLRP3 inflammasome. NLRP3 deletion increases mitophagy and protects against mitochondrial damage and neuroinflammation

induced by intermittent hypoxia through PINK1/Parkin-mediated mitophagy.<sup>39</sup> In this study, we found that NLRP3 KO significantly improve AR via upregulating PINK1/Parkin-mediated mitophagy. In addition, AR is generally considered a type 2 helper T (Th2) cells-driven disease.<sup>21</sup> In order to induce a Th2 response, HNEpCs were stimulated with IL-13. PINK1 siRNA inhibits PINK1/Parkin-mediated mitophagy and attenuates the beneficial effects of MCC950 on oxidative stress, inflammation, and apoptosis in IL-13-treated HNEpCs. However, the correlation between NLRP3 inflammasome and PINK1/Parkin-independent mitophagy in AR requires further exploration.

## Conclusion

This study revealed that inhibiting NLRP3 inflammasome activation improves AR via regulating PINK1/Parkin signaling pathway. The regulation of the NLRP3-mitophagy axis holds promise as a therapeutic strategy for AR.

## Abbreviations

AR, allergic rhinitis; IgE, immunoglobulin E; NLRP3, NOD-like receptor family pyrin domain-containing 3; IL-1 $\beta$ , interleukin-1 $\beta$ ; ROS, reactive oxygen species; PINK1, PTEN-induced putative kinase1; PARKIN, enzyme 3 (E3) ubiquitin ligase PRKN; WT, wild type; OVA, ovalbumin; ELISA, enzyme linked immunosorbent assay; OVA-sIgE, OVA-specific immunoglobulin E; TNF- $\alpha$ , tumor necrosis factor  $\alpha$ ; IFN- $\gamma$ , Interferon  $\gamma$ ; HE, hematoxylin-eosin; TB, toluidine blue; PAS, periodic acid-Schiff; GSH, glutathione; MDA, malondialdehyde; SOD, superoxide dismutase; MTROS, mitochondrial reactive oxygen species; BAX, BCL2 associated X protein; BCL-2, B-cell CLL/lymphoma 2; TOM20, outer mitochondrial membrane receptor Tom20; IF, immunofluorescence; IHC, Immunohistochemistry; TUNEL, terminal deoxynucleotidyl transferase dUTP nick end labeling; NC, negative control.

## Author Contributions

All authors contributed significantly to the work, whether that is in conception, study design, execution, data acquisition, analysis and interpretation, or across all these domains; participated in drafting, revising, or critically reviewing the article; provided final approval for publication; selected the journal for submission; and agree to be accountable for all aspects of the work.

## Funding

This study was financially supported by grants from the National Natural Science Foundation of China (grant number 81904165).

## Disclosure

The authors report no conflicts of interest in this work.

## References

1. Siddiqui ZA, Walker A, Pirwani MM, et al. Allergic rhinitis: diagnosis and management. *Br J Hosp Med*. 2022;83(2):1–9. doi:10.12968/hmed.2021.0570
2. Schuler Iv CF, Montejo JM. Allergic rhinitis in children and adolescents. *Immunol Allergy Clin North Am*. 2021;41(4):613–625. doi:10.1016/j.ia.2021.07.010
3. Bousquet J, Anto JM, Bachert C, et al. Allergic rhinitis. *Nat Rev Dis Primers*. 2020;6(1):95. doi:10.1038/s41572-020-00227-0
4. Cheng N, Wang Y, Gu Z. Understanding the role of NLRP3-mediated pyroptosis in allergic rhinitis: a review. *Biomed Pharmacother*. 2023;165:115203. doi:10.1016/j.biopha.2023.115203
5. Xu S, Wang D, Tan L, et al. The role of NLRP3 inflammasome in type 2 inflammation related diseases. *Autoimmunity*. 2024;57(1):2310269. doi:10.1080/08916934.2024.2310269
6. Leszczynska K, Jakubczyk D, Gorska S. The NLRP3 inflammasome as a new target in respiratory disorders treatment. *Front Immunol*. 2022;13:1006654. doi:10.3389/fimmu.2022.1006654
7. Kelley N, Jeltama D, Duan Y, et al. The NLRP3 Inflammasome: an overview of mechanisms of activation and regulation. *Int J Mol Sci*. 2019;20(13):3328. doi:10.3390/ijms20133328
8. Zhang B, Pan C, Feng C, et al. Role of mitochondrial reactive oxygen species in homeostasis regulation. *Redox Rep*. 2022;27(1):45–52. doi:10.1080/13510002.2022.2046423
9. Su L, Zhang J, Gomez H, et al. Mitochondria ROS and mitophagy in acute kidney injury. *Autophagy*. 2023;19(2):401–414. doi:10.1080/15548627.2022.2084862

10. Zhao Y, Qiu C, Wang W, et al. Cortistatin protects against intervertebral disc degeneration through targeting mitochondrial ROS-dependent NLRP3 inflammasome activation. *Theranostics*. 2020;10(15):7015–7033. doi:10.7150/thno.45359
11. Lu Y, Li Z, Zhang S, et al. Cellular mitophagy: mechanism, roles in diseases and small molecule pharmacological regulation. *Theranostics*. 2023;13(2):736–766. doi:10.7150/thno.79876
12. Han R, Liu Y, Li S, et al. PINK1-PRKN mediated mitophagy: differences between in vitro and in vivo models. *Autophagy*. 2023;19(5):1396–1405. doi:10.1080/15548627.2022.2139080
13. Liu S, Wang C, Zhang Y, et al. Polydatin inhibits mitochondrial damage and mitochondrial ROS by promoting PINK1-Parkin-mediated mitophagy in allergic rhinitis. *FASEB J*. 2023;37:e22852.
14. Lin Q, Li S, Jiang N, et al. Inhibiting NLRP3 inflammasome attenuates apoptosis in contrast-induced acute kidney injury through the upregulation of HIF1A and BNIP3-mediated mitophagy. *Autophagy*. 2021;17(10):2975–2990. doi:10.1080/15548627.2020.1848971
15. Yu W, Du J, Peng L, et al. ROR $\alpha$  overexpression reduced interleukin-33 expression and prevented mast cell degranulation and inflammation by inducing autophagy in allergic rhinitis. *Immun Inflamm Dis*. 2023;11(10):e1017. doi:10.1002/iid3.1017
16. Yu JI, Kim JH, Nam KE, et al. Pneumococcal  $\Delta$  pep27 immunization attenuates TLRs and NLRP3 expression and relieves murine ovalbumin-induced allergic rhinitis. *J Microbiol Biotechnol*. 2022;32(6):709–717. doi:10.4014/jmb.2203.03006
17. Zhou H, Zhang W, Qin D, et al. Activation of NLRP3 inflammasome contributes to the inflammatory response to allergic rhinitis via macrophage pyroptosis. *Int Immunopharmacol*. 2022;110:109012. doi:10.1016/j.intimp.2022.109012
18. Bai X, Liu P, Shen H, et al. Water-extracted *Lonicera japonica* polysaccharide attenuates allergic rhinitis by regulating NLRP3-IL-17 signaling axis. *Carbohydr Polym*. 2022;297:120053. doi:10.1016/j.carbpol.2022.120053
19. Zhang H, Zhu X, Liu H, et al. Long non coding RNA FOXD3-AS1 alleviates allergic rhinitis by elevating the Th1/Th2 ratio via the regulation of dendritic cells. *Immunol Invest*. 2023;52(4):499–512. doi:10.1080/08820139.2023.2197940
20. Liu P, Hu T, Kang C, et al. Research advances in the treatment of allergic Rhinitis by probiotics. *J Asthma Allergy*. 2022;15:1413–1428. doi:10.2147/JAA.S382978
21. Zhang Y, Lan F, Zhang L. Update on pathomechanisms and treatments in allergic rhinitis. *Allergy*. 2022;77(11):3309–3319. doi:10.1111/all.15454
22. Dong F, Tan J, Zheng Y. Chlorogenic acid alleviates allergic inflammatory responses through regulating Th1/Th2 Balance in ovalbumin-induced allergic rhinitis mice. *Med Sci Monit*. 2020;26:e923358. doi:10.12659/MSM.923358
23. Zoabi Y, Levi-Schaffer F, Eliashar R. Allergic Rhinitis: pathophysiology and treatment focusing on mast cells. *Biomedicines*. 2022;10(10):2486. doi:10.3390/biomedicines10102486
24. Liu R, Zhang Y, Wang Y, et al. Anti-inflammatory effect of dictamnine on allergic rhinitis via suppression of the LYN kinase-mediated molecular signaling pathway during mast cell activation. *Phytother Res*. 2023;37(9):4236–4250. doi:10.1002/ptr.7904
25. Drazdauskaitė G, Layhadi JA, Shamji MH. Mechanisms of allergen immunotherapy in allergic Rhinitis. *Curr Allergy Asthma Rep*. 2020;21(1):2. doi:10.1007/s11882-020-00977-7
26. Burchett JR, Dailey JM, Kee SA, et al. Targeting mast cells in allergic disease: current therapies and drug repurposing. *Cells*. 2022;11(19):3031. doi:10.3390/cells11193031
27. Jiang Y, Nguyen TV, Jin J, et al. Bergapten ameliorates combined allergic rhinitis and asthma syndrome after PM2.5 exposure by balancing Treg/Th17 expression and suppressing STAT3 and MAPK activation in a mouse model. *Biomed Pharmacother*. 2023;164:114959. doi:10.1016/j.biopha.2023.114959
28. Choi S, Jung MA, Hwang YH, et al. Anti-allergic effects of *Asarum heterotropoides* on an ovalbumin-induced allergic rhinitis murine model. *Biomed Pharmacother*. 2021;141:111944. doi:10.1016/j.biopha.2021.111944
29. Teleanu DM, Niculescu AG, Lungu II, et al. An overview of oxidative stress, neuroinflammation, and neurodegenerative diseases. *Int J Mol Sci*. 2022;23(11):5938. doi:10.3390/ijms23115938
30. Danevska IA, Jakjovska T, Zendelovska D, et al. Comparison of oxidative stress levels in healthy children and children with allergic Rhinitis. *Pril*. 2023;44(1):17–26. doi:10.2478/prilozi-2023-0003
31. Han M, Lee D, Lee SH, et al. Oxidative stress and antioxidant pathway in allergic Rhinitis. *Antioxidants*. 2021;11(1):10. doi:10.3390/antiox11010010
32. Liu X, Li M, Chen Z, et al. Mitochondrial calpain-I activates NLRP3 inflammasome by cleaving ATP5A1 and inducing mitochondrial ROS in CVB3-induced myocarditis. *Basic Res Cardiol*. 2022;117(1):40. doi:10.1007/s00395-022-00948-1
33. Qiu Z, He Y, Ming H, et al. Lipopolysaccharide (LPS) aggravates high glucose- and hypoxia/reoxygenation-induced injury through activating ROS-dependent NLRP3 inflammasome-mediated pyroptosis in H9C2 cardiomyocytes. *J Diabetes Res*. 2019;2019:8151836. doi:10.1155/2019/8151836
34. Li Y, Sun L, Zhang Y. Programmed cell death in the epithelial cells of the nasal mucosa in allergic rhinitis. *Int Immunopharmacol*. 2022;112:109252. doi:10.1016/j.intimp.2022.109252
35. Ng MY, Wai T, Simonsen A. Quality control of the mitochondrion. *Dev Cell*. 2021;56(7):881–905. doi:10.1016/j.devcel.2021.02.009
36. Onishi M, Yamano K, Sato M, et al. Molecular mechanisms and physiological functions of mitophagy. *EMBO J*. 2021;40(3):e104705. doi:10.15252/embj.2020104705
37. Qiu WQ, Ai W, Zhu FD, et al. Polygala saponins inhibit NLRP3 inflammasome-mediated neuroinflammation via SHP-2-mediated mitophagy. *Free Radic Biol Med*. 2022;179:76–94. doi:10.1016/j.freeradbiomed.2021.12.263
38. Lin Q, Li S, Jiang N, et al. PINK1-parkin pathway of mitophagy protects against contrast-induced acute kidney injury via decreasing mitochondrial ROS and NLRP3 inflammasome activation. *Redox Biol*. 2019;26:101254. doi:10.1016/j.redox.2019.101254
39. Wu X, Gong L, Xie L, et al. NLRP3 deficiency protects against intermittent hypoxia-induced neuroinflammation and mitochondrial ROS by promoting the PINK1-parkin pathway of mitophagy in a murine model of sleep apnea. *Front Immunol*. 2021;12:628168. doi:10.3389/fimmu.2021.628168

Journal of Asthma and Allergy

Dovepress

### Publish your work in this journal

The Journal of Asthma and Allergy is an international, peer-reviewed open-access journal publishing original research, reports, editorials and commentaries on the following topics: Asthma; Pulmonary physiology; Asthma related clinical health; Clinical immunology and the immunological basis of disease; Pharmacological interventions and new therapies. The manuscript management system is completely online and includes a very quick and fair peer-review system, which is all easy to use. Visit <http://www.dovepress.com/testimonials.php> to read real quotes from published authors.

Submit your manuscript here: <https://www.dovepress.com/journal-of-asthma-and-allergy-journal>